Production of charged pions, kaons and protons at large transverse momenta in pp and Pb–Pb collisions at √sNN = 2.76 TeV

(ALICE Collaboration) Abelev, B.; ...; Antičić, Tome; ...; Gotovac, Sven; ...; Mudnić, Eugen; ...; Planinić, Mirko; ...; ...

Physics Letters B 736 (2014) 196–207

Contents lists available at ScienceDirect

Physics Letters B

www.elsevier.com/locate/physletb

Production of charged pions, kaons and protons at large transverse momenta in pp and Pb–Pb collisions at $\sqrt{s_{\mathrm{NN}}} = 2.76$ TeV

ALICE Collaboration *

ARTICLE INFO

Article history:
Received 15 May 2014
Received in revised form 27 June 2014
Accepted 7 July 2014
Available online 15 July 2014
Editor: L. Rolandi

Keywords:
Identified particle production
High p_{T}
Particle ratios
Baryon anomaly
Nuclear modification factor
ALICE
LHC

ABSTRACT

Transverse momentum spectra of $\pi^{\pm}$, $\mathrm{K}^{\pm}$ and $\mathrm{p}(\bar{\mathrm{p}})$ up to $p_{\mathrm{T}} = 20$ GeV/c at mid-rapidity in pp, peripheral (60–80%) and central (0–5%) Pb–Pb collisions at $\sqrt{s_{\mathrm{NN}}} = 2.76$ TeV have been measured using the ALICE detector at the Large Hadron Collider. The proton-to-pion and the kaon-to-pion ratios both show a distinct peak at $p_{\mathrm{T}} \approx 3$ GeV/c in central Pb–Pb collisions. Below the peak, $p_{\mathrm{T}} < 3$ GeV/c, both ratios are in good agreement with hydrodynamical calculations, suggesting that the peak itself is dominantly the result of radial flow rather than anomalous hadronization processes. For $p_{\mathrm{T}} > 10$ GeV/c particle ratios in pp and Pb–Pb collisions are in agreement and the nuclear modification factors for $\pi^{\pm}$, $\mathrm{K}^{\pm}$ and $\mathrm{p}(\bar{\mathrm{p}})$ indicate that, within the systematic and statistical uncertainties, the suppression is the same. This suggests that the chemical composition of leading particles from jets in the medium is similar to that of vacuum jets.

1. Introduction

Heavy-ion collisions at ultra relativistic energies produce a new form of QCD matter characterized by the deconfined state of quarks and gluons (partons). Measurements of the production of identified particles in Pb–Pb collisions, relative to pp collisions, provide information about the dynamics of this dense matter. In pp collisions, high transverse momentum ($p_{\mathrm{T}} > 2$ GeV/c) hadrons are produced from fragmentation of jets that can be calculated folding the perturbative QCD calculations for jets with universal fragmentation functions determined from data such as those reported here. The bulk production of particles at lower p_{T} is non-perturbative and requires phenomenological modeling. In heavy-ion collisions the production can be affected by the medium in several different ways. In particular there is an intermediate transverse momentum regime, $2 < p_{\mathrm{T}} < 8$ GeV/c, where the baryon-to-meson ratios, *e.g.* the proton yield divided by the pion yield, measured by experiments at RHIC revealed a, so far, not well understood enhancement [1–3]. This so-called "baryon anomaly" could indicate the presence of new hadronization mechanisms such as parton recombination [4–6] that could be significantly enhanced and/or extended out to higher p_{T} at LHC due to larger mini-jet production [7]. For transverse momenta above 10 GeV/c one expects to be able to study the pure energy loss (jet quenching) of high p_{T} scattered partons traversing the medium [8–10]. This affects the inclusive charged particle p_{T} spectrum as has been seen at RHIC [11,12] and over an extended p_{T} range, up to 100 GeV/c, at the LHC [13,14]. The additional information provided by particle identification (PID) is of fundamental interest to study the differences in the dynamics of fragmentation between quarks and gluons to baryons and mesons [15], and also to study the differences in their interaction with the medium considering that, due to the color Casimir factor, gluons lose a factor of two more energy than quarks [16,17]. The results presented in this Letter address three open experimental questions: Are there indications that the kaons are affected by radial flow at intermediate p_{T}? Does the baryon-to-meson ratio return to the pp value for high p_{T} (>10 GeV/c) as suggested by the recent publication of the $\Lambda/\mathrm{K}^0_{\mathrm{S}}$ ratio [18]? Are there large particle species dependent jet quenching effects as predicted in several models [19–21], where measurements at RHIC, in particular for baryons, are inconclusive due to the limited p_{T}-range and the large systematic and statistical uncertainties [22–24]?

2. Data analyses

In this Letter we present the measurement of the production of pions (kaons and protons) from a p_{T} of a few hundred MeV/c up to $p_{\mathrm{T}} = 20$ GeV/c in $\sqrt{s_{\mathrm{NN}}} = 2.76$ TeV pp and Pb–Pb collisions with the ALICE detector [25]. The Inner Tracking System (ITS) and the Time Projection Chamber (TPC) are used for vertex finding and tracking. The ITS and TPC also provide PID through the measurement of the specific energy loss, $\mathrm{d}E/\mathrm{d}x$. The PID is further

* alice-publications@cern.ch.

http://dx.doi.org/10.1016/j.physletb.2014.07.011

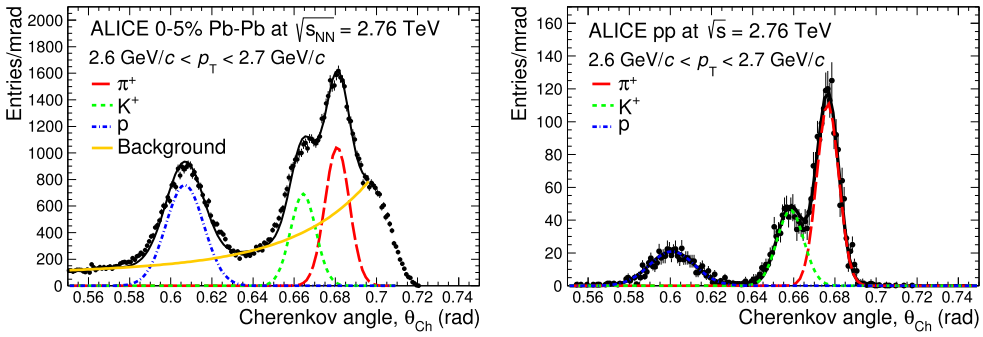

Fig. 1. (Color online.) Distributions of the Cherenkov angle measured in the HMPID for positive tracks in a narrow p_T bin, for 0–5% central Pb–Pb (left) and pp (right) collisions. The slight shift of the pions, kaons and protons peaks in Pb–Pb data compared to the pp ones is due to different data taking conditions of the HMPID Cherenkov radiator (liquid C_6F_{14}).

Table 1
The η/y and p_T range (GeV/c) covered by each analysis.

Analysis	η/y range	π	K	p
ITS-sa	$\|y\| < 0.5$	0.1–0.7	0.2–0.55	0.3–0.6
TPC–TOF	$\|y\| < 0.5$	0.3–1.2	0.3–1.2	0.45–2.0
TOF	$\|y\| < 0.5$	0.5–2.5	0.5–2.4	0.8–3.8
HMPID	$\|y\| < 0.5$	1.5–4.0	1.5–4.0	1.5–6.0
High p_T dE/dx	$\|\eta\| < 0.8$	2.0–20.0	3.0–20.0	3.0–20.0

improved at low and intermediate p_T using the Time-of-Flight (TOF) and the High Momentum PID (HMPID) Cherenkov detectors. In Pb–Pb collisions the spectra at low p_T have already been published [26] and the new addition here is the extension of the p_T range up to 20 GeV/c and the improvement at intermediate p_T for the 0–40% most central collisions using the HMPID. The pp low p_T analysis combining information from ITS, TPC, and TOF follows the same procedures as the ones published by ALICE at $\sqrt{s} = 900$ GeV [27] and in $\sqrt{s_{NN}} = 2.76$ TeV Pb–Pb collisions [26]. The main focus in the following will therefore be on explaining the analysis details for the HMPID and the high p_T dE/dx analysis.

The pp analyses use 40×10^6 and the Pb–Pb minimum bias analysis uses 11×10^6 collision events. The HMPID analysis used the 2011 centrality triggered Pb–Pb data with around 4.1×10^6 0–5% central collision events. Data were taken during 2010 and 2011 under conditions where pileup effects were negligible. Minimum bias interactions are triggered based on the signals from forward scintillators (V0) and, in pp collisions, the two innermost silicon pixel layers of the ITS (SPD). The trigger efficiency is 88.1% for pp inelastic collisions [28] and 97.1% for non-diffractive Pb–Pb collisions [29]. The Pb–Pb collision centrality is determined from the measured amplitude in the V0 detector [30] which is related to the number of participating nucleons and the nuclear overlap function (T_{AA}) through simulations based on a Glauber model [29]. The same event and track selection is used as in the inclusive charged particle analysis [31]. Track cuts are optimized in order to select primary charged particles in the pseudorapidity range $|\eta| < 0.8$ and all results presented in this paper are corrected for feed-down from weak decays. As listed in Table 1 the low p_T analysis is done for $|y| < 0.5$, while the high p_T analysis is done for $|\eta| < 0.8$, to take advantage of the full statistics, and the final spectra are then normalized to the corresponding rapidity intervals, see Eq. (1) below.

2.1. Identified particle spectra at low p_T

The pp low p_T analysis relies on the combination of four almost independent PID techniques, named after the detectors involved: ITS-sa, TPC–TOF, TOF and HMPID. The techniques have complementary p_T ranges listed in Table 1.

The ITS-sa analysis exploits stand-alone (sa) tracks reconstructed in the ITS to be able to go as low in p_T as possible. The identification is done based on dE/dx measurements in up to 4 of the 6 silicon layers. This information is combined in a Bayesian approach using a set of priors determined with an iterative procedure, and the track identity is assigned according to the highest probability. The minor residual contamination due to misidentification is less than 10% in the p_T-range reported in Table 1 and corrected for using MC.

The other three analyses all use global tracks reconstructed in both the ITS and the TPC. The TPC–TOF analysis is optimized to combine the information from the TPC and TOF. The identification is based on a three standard deviations agreement with the expected detector signal and resolution (3σ) in the TPC dE/dx and for $p_T > 0.6$ GeV/c a 3σ requirement is also applied for the time-of-flight provided by the TOF detector. The TOF analysis identifies particles comparing the measured time-of-flight from the primary vertex to the TOF detector, t_{tof}, and the time expected under a given mass hypothesis, t_i^{exp} ($i = \pi, K, p$). The TOF standalone analysis is optimized for handling momentum regions where the separation is challenging. The precise signal shape for $t_{tof} - t_i^{exp}$, including an exponential tail, is used, and the yield in a given p_T interval is obtained by fitting.

The HMPID [32,33] is designed as a single-arm proximity-focusing Ring Imaging CHerenkov (RICH) detector where the radiator is a 15 mm thick layer of liquid C_6F_{14} (perfluorohexane). It is located at about 5 m from the beam axis, covering a limited acceptance of $|\eta| < 0.55$ and $1.2^\circ < \varphi < 58.5^\circ$. The PID in the HMPID is done by measuring the Cherenkov angle, θ_{ch}. In the reconstruction, the tracks are propagated to the HMPID detector and associated with a MIP signal. A Hough Transform Method (HTM) [34] is used to discriminate the signal from the background. For a given track, the mean Cherenkov angle is computed as the weighted average of the single photon angles selected by the HTM. The Cherenkov angle distribution is then fitted to obtain the yields, see Fig. 1 for an example of fits in the Pb–Pb and pp analysis.

The raw yields measured by each analysis are corrected for the reconstruction, selection, PID efficiency, and misidentification probability. The contamination due to particles from weak decays of light flavor hadrons and interactions with the material is subtracted using MC-template fits of the distance-of-closest approach distributions [26]. Finally the raw spectra are corrected for the detector acceptance, trigger selection, vertex and track reconstruction efficiency.

The systematic uncertainties for the ITS, TPC, and TOF analyses are obtained in essentially the same way as reported in [27,26]. The systematic uncertainty for the HMPID analysis has contributions from tracking and PID. These uncertainties have been estimated by changing individually the track selection cuts and the

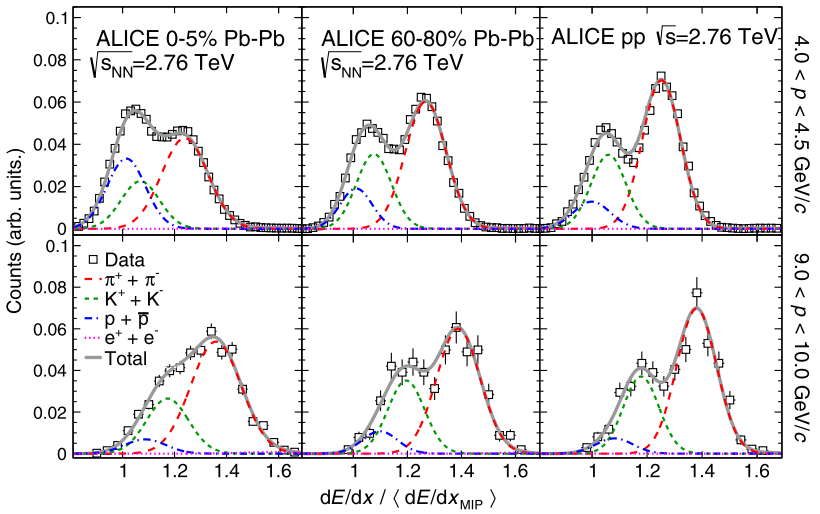

Fig. 2. (Color online.) $\mathrm{d}E/\mathrm{d}x$ distributions measured for $|\eta| < 0.2$ and normalized to the integrated yields. The signals are fitted to a sum of four Gaussian functions (solid line). Two p intervals are shown for central (left) and peripheral (center) Pb–Pb; and pp (right) collisions. In all momentum intervals the electron fraction is below 1% (not visible). Individual yields are shown as dashed curves; protons in blue (left), kaons in green, and pions in red (right).

parameters of the fit function used to extract the raw yields by ±10%. In addition, the uncertainty of the association of the track to the MIP signal is obtained by varying the value of the distance cut required for the match.

The HMPID analysis in Pb–Pb collisions is analogous to the pp analysis except for the treatment of the background. In central Pb–Pb collisions, where the total number of hits in the HMPID chambers is large, it is possible that a Cherenkov ring is constructed based on hits incorrectly associated with the track. Fig. 1 gives examples of the reconstructed Cherenkov angle distributions in a narrow p_{T} interval. In pp collisions (right panel) the reconstructed angle distribution is fitted by a sum of three Gaussian distributions, corresponding to the signals from pions, kaons and protons. In the case of Pb–Pb collisions (left panel) the additional background distribution is modeled with a 6th order polynomial found to minimize the reduced χ^2 of the fit. The shoulder in the background distribution starting at 0.7 rad is a boundary effect due to the finite chamber geometrical acceptance that is also observed in MC simulations. The fitting is done in two steps, where the width and the mean of each Gaussian distribution are free parameters in the first step and are then used to obtain a p_{T} dependent parameterization. This parameterization is used to constrain the parameters in the second final fit. The means and widths constrained in this way are found to be independent of centrality. Finally we note that the background increases with the Cherenkov angle because the fiducial area used in the reconstruction becomes larger, making it more likely to associate spurious hits with the signal.

The PID efficiency has been evaluated from a Monte Carlo simulation that reproduces well the background in the data. A data-driven cross check of the efficiency has been performed using a clean sample of protons and pions from Λ and $\mathrm{K}^0_{\mathrm{S}}$ decays identified in the TPC based on their topological decay.

To estimate the uncertainty due to the incomplete knowledge of the shape of the background distribution, an alternative background function, depending on $\tan(\theta_{\mathrm{ch}})$ and derived from geometrical considerations in case of orthogonal tracks [32], has been used. The corresponding systematic uncertainty reaches the maximum value at low momenta for the most central collisions (∼15% for pions, and ∼8% for kaons and protons). The systematic uncertainty decreases with p_{T} as the track inclination angle in the bending plane decreases so that the fiducial area for the Cherenkov pattern search is smaller.

2.2. Identified particle spectra at high p_{T}

Particle identification is performed in the relativistic rise regime of the Bethe–Bloch (BB) curve where the $\langle \mathrm{d}E/\mathrm{d}x \rangle$ separation between particles with different masses is nearly constant [35]. The $\mathrm{d}E/\mathrm{d}x$ is obtained as the truncated mean of the 0–60% lowest charge samples associated with the track in the TPC [36]. The $\mathrm{d}E/\mathrm{d}x$ response depends on the track length so the analysis is done in four equally sized $|\eta|$-intervals, and a geometrical cut to remove tracks entering the gap in between the TPC readout chambers is applied to select tracks with the best $\mathrm{d}E/\mathrm{d}x$ resolution. The separation in number of standard deviations (σ) between pions and kaons (pions and protons) in pp and peripheral Pb–Pb collision is around 3.2 (4.6) at momentum $p \approx 6$ GeV/c for $0.6 < |\eta| < 0.8$ where the separation is largest. In central Pb–Pb collisions one finds a separation of 2.4σ (3.5σ). In the worst case, $|\eta| < 0.2$, the separation is 11–15% smaller.

Fig. 2 shows examples of the $\mathrm{d}E/\mathrm{d}x$ spectra obtained for pp and Pb–Pb (central and peripheral) collisions for two momentum, p, intervals and $|\eta| < 0.2$ where $p \approx p_{\mathrm{T}}$. The pion, kaon, and proton yields are extracted by fitting a sum of four Gaussian functions (including electrons) to the $\mathrm{d}E/\mathrm{d}x$ spectra.[1] To reduce the degrees of freedom in the fits from 12 to 4, parameterizations of the BB ($\langle \mathrm{d}E/\mathrm{d}x \rangle$) and resolution ($\sigma$) curves as a function of $\beta\gamma$ are extracted first using tracks from identified particles. Samples of secondary pions ($30 < \beta\gamma < 50$) and protons ($3 < \beta\gamma < 7$) are obtained through the reconstruction of the weak-decay topology of $\mathrm{K}^0_{\mathrm{S}}$ and Λ, respectively; a similar algorithm is used to identify electrons resulting from photon conversions (fixing the $\mathrm{d}E/\mathrm{d}x$ plateau: $\beta\gamma > 1000$). Finally, using information from the time-of-flight detector the relative pion content can be enhanced for sub-samples of the full datasets ($16 < \beta\gamma < 50$).

The $\langle \mathrm{d}E/\mathrm{d}x \rangle$ separation between kaons and protons in the high p_{T} analysis is smallest for $p \approx 3$ GeV/c and increases with p until both species are on the relativistic rise [35]. In central collisions the $\langle \mathrm{d}E/\mathrm{d}x \rangle$ separation is the lowest and the systematic uncertainties on the extracted yields are correspondingly large as discussed later, see Table 2. Hence, to improve the central val-

[1] We note that muons from heavy flavor decays are subtracted from the pions based on the measured electron yields and that contamination from deuterons and tritons are negligible (≪1%).

Table 2
Systematic uncertainties, separated into the N_{ch}, PID, and efficiency part, on the invariant yields from $3 < p_T < 4$ GeV/c (left quoted value) to $10 < p_T < 20$ GeV/c (right quoted value).

System	Pb–Pb 0–5%	Pb–Pb 60–80%	pp
N_{ch}[a]	8.3–8.2%	9.9–9.8%	7.4–7.6%
$\pi^+ + \pi^-$[b]	1.7–2.4%	1.5–2.2%	1.2–1.7%
$K^+ + K^-$	19–7.9%	17–8.7%	16–5.7%
$p + \bar{p}$	9.9–21%	20–24%	24–20%
Efficiency ratios[c]		3%	

[a] Taken directly from [31].
[b] Additional contribution due to $\mu^{\pm}$ contamination is $\leq$1%.
[c] Same for all centralities and all particle species.

ues for the kaons and protons, the K^0_S yields [18] are used as a proxy for the charged kaons to further constrain the BB curve in Pb–Pb collisions in a procedure which uses a two dimensional fit of dE/dx vs momentum. The effect of the K^0_S bias is only relevant in central collisions at low p_T (<4 GeV/c). At 3 GeV/c the effect on the extracted kaon yield is an increase of 10% (<1%) for 0–5% (60–80%) collision centrality.

With the above information the BB and the resolution curves are determined for kaons and protons in the full momentum interval reported here and for pions with $p < 7$ GeV/c. For $p > 7$ GeV/c the pion $\langle dE/dx \rangle$ is restricted by the logarithmic rise until the $\langle dE/dx \rangle$ starts to approach the plateau. This lack of additional constraint currently limits the p_T reach of the analysis to ~20 GeV/c.

From the fits in Fig. 2 the particle fractions, $f_{\pi/K/p}(p)$ are extracted. The fraction in a p_T bin, $f_{\pi/K/p}(p_T)$, is obtained as the weighted average of the contributing momentum (p) bins. The p_T-dependent fractions are found to be independent of η and so all four η regions are averaged.

Finally, the invariant yields are obtained using the p_T spectrum for inclusive charged particles [31], $\frac{d^2N_{ch}}{dp_T d\eta}$, in the following way:

$$\frac{d^2N_{\pi/K/p}}{dp_T dy} = J_{\pi/K/p} \frac{d^2N_{ch}}{dp_T d\eta} \frac{\epsilon_{ch}}{\epsilon_{\pi/K/p}} f_{\pi/K/p}(p_T), \quad (1)$$

where (ϵ_{ch}) $\epsilon_{\pi/K/p}$ is the efficiency for (un)identified particles and $J_{\pi/K/p}$ is the Jacobian correction (from η to y). Normalizing to the p_T spectrum of inclusive charged particles guarantees that only the systematic uncertainty due to PID is relevant when comparing the modification of the p_T spectra of π/K/p to those for the unidentified particles. The p_T resolution is around 5% at $p_T = 20$ GeV/c and the p_T spectra have been corrected for this resolution using an unfolding procedure for $p_T > 10$ GeV/c [31,37]. This correction is less than 2% at $p_T = 20$ GeV/c.

2.2.1. Systematic uncertainties

The systematic uncertainty on the invariant yields has three main components: event and track selection, efficiency correction of the fractions, and the fraction extraction. Contributions from the event and track selection are taken directly from the inclusive charged particle analysis [31]. Efficiency ratios ($\epsilon_{ch}/\epsilon_{\pi/K/p}$) are found to be nearly independent of p_T (a small dependence is only observed for kaons), similar for all systems, and model independent within 3%. The largest systematic uncertainty in the extraction of the fractions comes from the uncertainty in the constrained parameters: the means ($\langle dE/dx \rangle$) and the widths (σ) used in the fits. The uncertainty on these parameters are estimated from the average difference between the final parameterizations and the data points obtained from the enhanced samples with identified particles. In addition, the statistical uncertainty on the extracted BB parameterization in peripheral Pb–Pb collisions is found to be of a similar magnitude and also taken into account in the following variations. The dE/dx spectra are then refitted, varying the means and the widths within the estimated uncertainties, and the variation of the fractions are assigned as systematic errors. In this way the correlations in the systematic uncertainty for the particle ratios can be directly included. A summary of the PID systematic uncertainties is shown in Table 2. The N_{ch} systematic uncertainties cancel in the particle ratios.

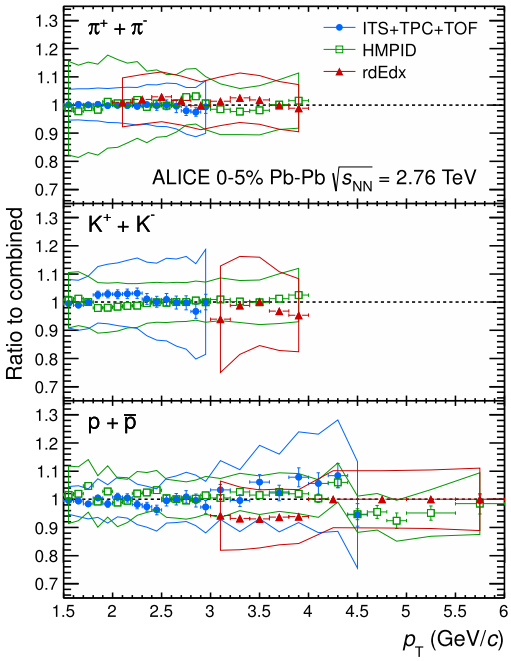

Fig. 3. (Color online.) The ratio of individual spectra to the combined spectrum as a function of p_T for pions (top), kaons (center), and protons (bottom). Only the p_T-range where the analyses overlap is shown. The ITS + TPC + TOF spectra are the results published in [26]. The statistical and independent systematic uncertainties are shown as vertical error bars and as a band, respectively, and only include those on the individual spectra.

3. Results and discussion

The measurement of charged pion, kaon and (anti-)proton transverse momentum spectra has been performed via several independent analyses, each one focusing on a sub-range of the total p_T distribution, with emphasis on the individual detectors and specific techniques to optimize the signal extraction. The results were combined using the independent systematic uncertainties as weights in the overlapping ranges (a 3% common systematic uncertainty due to the TPC tracking is not in the weight but added directly to the combined spectrum). The statistical uncertainties are much smaller and therefore neglected in the combination weights. For $p_T > 4$ GeV/c only the high p_T analysis is used for all species. Fig. 3 shows the ratio of individual spectra to the combined spectrum for the 0–5% central Pb–Pb data, illustrating the compatibility between the different analyses.

Fig. 4 shows the invariant yields measured in Pb–Pb collisions compared to those in pp collisions scaled by the number of binary collisions, N_{coll} [29] obtained for the measured pp cross section [28]. For peripheral Pb–Pb collisions the shapes of the invariant yields are similar to those observed in pp collisions. For central Pb–Pb collisions, the spectra exhibit a reduction in the production of high-p_T particles with respect to the reference which is characteristic of jet quenching.

Fig. 5 shows the proton-to-pion ratio, $(p + \bar{p})/(\pi^+ + \pi^-)$, as a function of p_T. For central (peripheral, not shown) Pb–Pb collisions it reaches ~0.83 (~0.35) at the maximum around 3 GeV/c

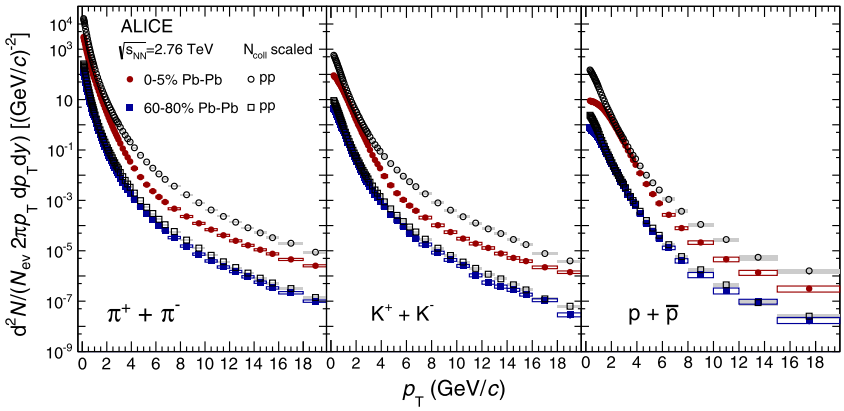

Fig. 4. (Color online.) Solid markers show the invariant yields of identified particles in central (circles) and peripheral (squares) Pb–Pb collisions. Open points show the pp reference yields scaled by the average number of binary collisions for 0–5% (circles) and 60–80% (squares) [29]. The statistical and systematic uncertainties are shown as vertical error bars and boxes, respectively.

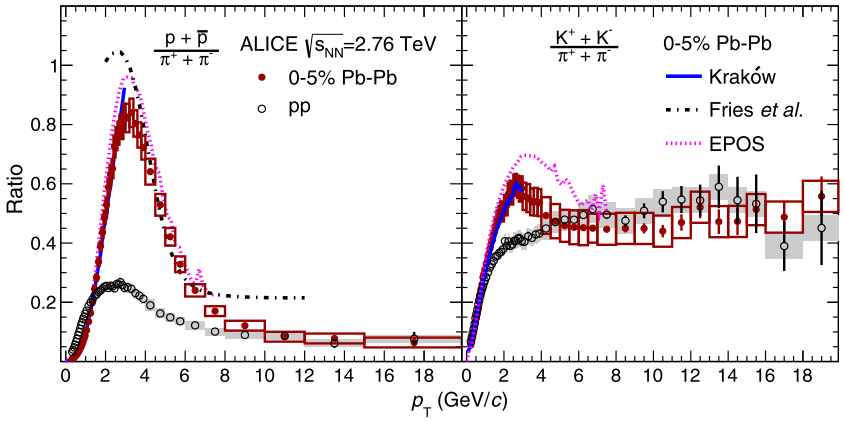

Fig. 5. (Color online.) Particle ratios as a function of p_T measured in pp and the most central, 0–5%, Pb–Pb collisions. Statistical and systematic uncertainties are displayed as vertical error bars and boxes, respectively. The theoretical predictions refer to Pb–Pb collisions, see text for references.

and then decreases with increasing p_T. These values are approximately 20% above the peak values measured by PHENIX [24] and STAR [22], when p/π^+ and $\bar{p}/\pi^-$ ratios are averaged and data are corrected for feed-down.

At LHC energies the mini-jet activity is expected to be larger than at RHIC energies, which motivated ratio predictions in the framework of recombination models where shower partons in neighboring jets can recombine to be an order of magnitude larger than the measurements reported here [7]. Other predictions where recombination only occurs for soft thermal radially flowing partons are, as shown in the figure, more consistent with the data [4]. The surprising new result is that in central Pb–Pb collisions the $(K^+ + K^-)/(\pi^+ + \pi^-)$ ratio also exhibits a bump at $p_T \approx 3$ GeV/c. This has not been observed at RHIC (this could be due to limitations in precision in this p_T region) but is also observed in the soft coalescence model [4]. The Kraków [38] hydrodynamical model captures the rise of both ratios quantitatively well, while a similar model, HKM [39] that is not shown, does slightly worse. The EPOS [40] event generator which has both hydrodynamics, but also the high p_T physics and special hadronization processes for quenched jets [41] qualitatively well describes the data but tends to overestimate the peaks. The recent result [42] that for $p_T < 3$ GeV/c the shape of the phi-to-pion ratio is consistent with the proton-to-pion ratio, reported here, taken together with the model comparisons shown in Fig. 5 indicate that the peak is mainly dominated by radial flow (the masses of the hadrons).

For higher p_T (>10 GeV/c) both particle ratios behave like those in pp, suggesting that fragmentation dominates the hadron production. In this p_T regime, the particle ratios in pp are not well described by the pQCD calculations in [43]. It was recently shown [44] that in general the fragmentation functions for gluons are badly constrained, leading to disagreement of up to a factor 2 with N_{ch} spectra measured at LHC. Furthermore it was pointed out that data with $p_T > 10$ GeV/c, as reported here, are needed to reduce the scale dependence that seems to be the origin of the disagreement.

Fig. 6 shows the nuclear modification factor R_{AA} as a function of p_T defined as the ratio of the Pb–Pb spectra to the N_{coll} scaled pp spectra shown in Fig. 4. The R_{AA} for the sum of kaons and protons is included as it allows the most precise quantitative comparison to the R_{AA} of pions. For $p_T < 10$ GeV/c protons appear to be less suppressed than kaons and pions, consistent with the particle ratios shown in Fig. 5. At larger p_T (>10 GeV/c) all particle species are equally suppressed; so despite the strong energy loss observed in the most central heavy-ion collisions, the particle composition and ratios at high p_T are similar to those in vacuum.

The models cited in the introduction all suggest large differences, of 50% or more, between the suppression of different species that are either related to mass ordering or baryon-vs-meson effects. The differences are naturally large in these scenarios because they are directly related to the large suppression. To quantify the similarity of the suppression the double R_{AA} ratios, *e.g.* $R_{AA}^{p+\bar{p}}/R_{AA}^{\pi^+ + \pi^-}$, are inspected. Fig. 7 shows the double ratios constructed using the particle ratios to properly handle that the dominant correlated systematic uncertainties are between particle species and not between different collision systems. We

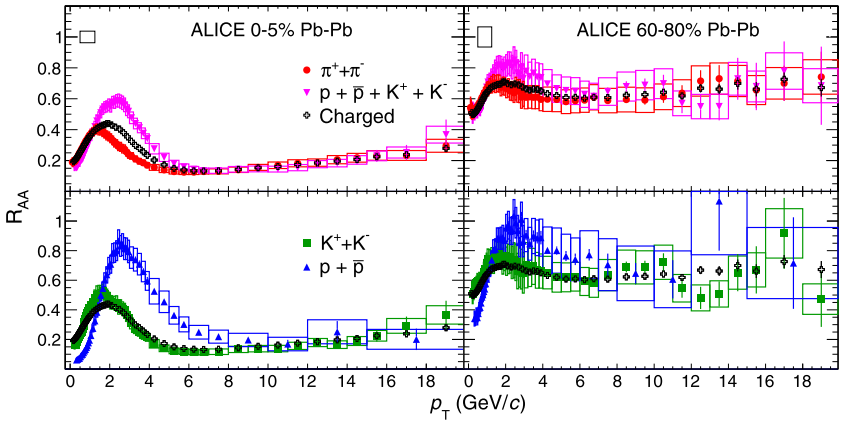

Fig. 6. (Color online.) The nuclear modification factor R_{AA} as a function of p_T for different particle species. Results for 0–5% (left) and 60–80% (right) collision centralities are shown. Statistical and systematic uncertainties are plotted as vertical error bars and boxes around the points, respectively. The total normalization uncertainty (pp and Pb–Pb) is indicated by the black boxes in the top panels [31].

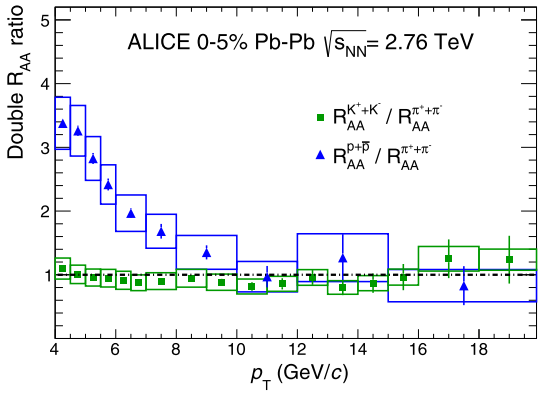

Fig. 7. (Color online.) R_{AA} double ratios as a function of p_T for $p_T > 4$ GeV/c. Statistical and PID systematic uncertainties are plotted as vertical error bars and boxes around the points, respectively.

note that a similar ratio for protons and pions made with the STAR data [22,23] would give a flat ratio for $p_T > 3$ GeV/c of approximately 3 ± 2. The results disfavor significant modifications of hadro-chemistry within the hard core of jets, as predicted based on medium modified color flow which introduces a mass ordering of the fragmentation [19], or due to changes in the color structure of the quenched probe which could enhance baryon production [20]. The data also contradict predictions where fragmentation into color neutral hadrons, assumed to have no energy loss after formation, occurs in the medium and the formation time scales directly with the hadron mass [21].

4. Conclusions

The production of pions, kaons and protons has been measured in pp and central and peripheral Pb–Pb collisions up to high p_T. From the invariant yields we derived the particle ratios and the R_{AA} as a function of p_T. We observe that the proton-to-pion and the kaon-to-pion ratios both exhibit a peak and that at low p_T the rise of both ratios can be well described by hydrodynamic calculations. This rules out models where shower partons recombine and sets strong constraints for soft recombination models. At higher-p_T, both ratios are compatible with those measured in pp collisions. From the nuclear modification factor R_{AA}, we conclude that for $p_T > 10$ GeV/c within the systematic and statistical uncertainties, pions, kaons and protons are suppressed equally. This rules out ideas in which the large energy loss leading to the suppression is associated with strong mass ordering or large fragmentation differences between baryons and mesons. The results presented here establish strong constraints on theoretical modeling for fragmentation and energy loss mechanisms.

Acknowledgements

The ALICE Collaboration would like to thank all its engineers and technicians for their invaluable contributions to the construction of the experiment and the CERN accelerator teams for the outstanding performance of the LHC complex.

The ALICE Collaboration gratefully acknowledges the resources and support provided by all Grid centres and the Worldwide LHC Computing Grid (WLCG) Collaboration.

The ALICE Collaboration acknowledges the following funding agencies for their support in building and running the ALICE detector: State Committee of Science, World Federation of Scientists (WFS) and Swiss Fonds Kidagan, Armenia; Conselho Nacional de Desenvolvimento Científico e Tecnológico (CNPq), Financiadora de Estudos e Projetos (FINEP), Fundação de Amparo à Pesquisa do Estado de São Paulo (FAPESP); National Natural Science Foundation of China (NSFC), the Chinese Ministry of Education (CMOE) and the Ministry of Science and Technology of China (MSTC); Ministry of Education and Youth of the Czech Republic; Danish Natural Science Research Council, the Carlsberg Foundation and the Danish National Research Foundation; The European Research Council under the European Community's Seventh Framework Programme; Helsinki Institute of Physics and the Academy of Finland; French CNRS-IN2P3, the 'Region Pays de Loire', 'Region Alsace', 'Region Auvergne' and CEA, France; German BMBF and the Helmholtz Association; General Secretariat for Research and Technology, Ministry of Development, Greece; Hungarian OTKA and National Office for Research and Technology (NKTH); Department of Atomic Energy and Department of Science and Technology of the Government of India; Istituto Nazionale di Fisica Nucleare (INFN) and Centro Fermi – Museo Storico della Fisica e Centro Studi e Ricerche "Enrico Fermi", Italy; MEXT Grant-in-Aid for Specially Promoted Research, Japan; Joint Institute for Nuclear Research, Dubna; National Research Foundation of Korea (NRF); CONACYT, DGAPA, México, ALFA-EC and the EPLANET Program (European Particle Physics Latin American Network); Stichting voor Fundamenteel Onderzoek der Materie (FOM) and the Nederlandse Organisatie voor Wetenschappelijk Onderzoek (NWO), Netherlands; Research Council of Norway (NFR); Polish Ministry of Science and Higher Education; National Science Centre, Poland; Ministry of National Education/Institute for Atomic Physics and CNCS-UEFISCDI – Romania; Ministry of Education and Science of Russian Federation, Russian Academy of Sciences, Russian Federal Agency of Atomic Energy, Russian Federal Agency for

Science and Innovations and The Russian Foundation for Basic Research; Ministry of Education of Slovakia; Department of Science and Technology, South Africa; CIEMAT, EELA, Ministerio de Economía y Competitividad (MINECO) of Spain, Xunta de Galicia (Consellería de Educación), CEADEN, Cubaenergía, Cuba, and IAEA (International Atomic Energy Agency); Swedish Research Council (VR) and Knut & Alice Wallenberg Foundation (KAW); Ukraine Ministry of Education and Science; United Kingdom Science and Technology Facilities Council (STFC); The United States Department of Energy, the United States National Science Foundation, the State of Texas, and the State of Ohio.

References

[1] K. Adcox, et al., Centrality dependence of π^+ / π^-, K^+ / K^-, p and anti-p production from $\sqrt{s_{NN}} = 130$ GeV Au+Au collisions at RHIC, Phys. Rev. Lett. 88 (2002) 242301, http://dx.doi.org/10.1103/PhysRevLett.88.242301, arXiv:nucl-ex/0112006.

[2] S. Adler, et al., Scaling properties of proton and anti-proton production in $\sqrt{s_{NN}} = 200$ GeV Au + Au collisions, Phys. Rev. Lett. 91 (2003) 172301, http://dx.doi.org/10.1103/PhysRevLett.91.172301, arXiv:nucl-ex/0305036.

[3] J. Adams, et al., Particle type dependence of azimuthal anisotropy and nuclear modification of particle production in Au + Au collisions at $\sqrt{s_{NN}} =$ 200 GeV, Phys. Rev. Lett. 92 (2004) 052302, http://dx.doi.org/10.1103/PhysRevLett.92.052302, arXiv:nucl-ex/0306007.

[4] R.J. Fries, B. Müller, C. Nonaka, S.A. Bass, Hadron production in heavy ion collisions: fragmentation and recombination from a dense parton phase, Phys. Rev. C 68 (2003) 044902, http://dx.doi.org/10.1103/PhysRevC.68.044902.

[5] V. Topor Pop, M. Gyulassy, J. Barrette, C. Gale, X. Wang, et al., Baryon junction loops in HIJING/B anti-B v2.0 and the baryon/meson anomaly at RHIC, Phys. Rev. C 70 (2004) 064906, http://dx.doi.org/10.1103/PhysRevC.70.064906, arXiv:nucl-th/0407095.

[6] S.J. Brodsky, A. Sickles, The Baryon anomaly: evidence for color transparency and direct hadron production at RHIC, Phys. Lett. B 668 (2008) 111–115, http://dx.doi.org/10.1016/j.physletb.2008.07.108, arXiv:0804.4608.

[7] R.C. Hwa, C. Yang, Proton enhancement at large p_T at LHC without structure in associated-particle distribution, Phys. Rev. Lett. 97 (2006) 042301, http://dx.doi.org/10.1103/PhysRevLett.97.042301, arXiv:nucl-th/0603053.

[8] M. Gyulassy, M. Plumer, Jet quenching in dense matter, Phys. Lett. B 243 (1990) 432–438, http://dx.doi.org/10.1016/0370-2693(90)91409-5.

[9] M. Gyulassy, X.-n. Wang, Multiple collisions and induced gluon Bremsstrahlung in QCD, Nucl. Phys. B 420 (1994) 583–614, http://dx.doi.org/10.1016/0550-3213(94)90079-5, arXiv:nucl-th/9306003.

[10] E. Wang, X.-N. Wang, Jet tomography of dense and nuclear matter, Phys. Rev. Lett. 89 (2002) 162301, http://dx.doi.org/10.1103/PhysRevLett.89.162301, arXiv:hep-ph/0202105.

[11] K. Adcox, et al., Formation of dense partonic matter in relativistic nucleus–nucleus collisions at RHIC: experimental evaluation by the PHENIX collaboration, Nucl. Phys. A 757 (2005) 184–283, http://dx.doi.org/10.1016/j.nuclphysa.2005.03.086, arXiv:nucl-ex/0410003.

[12] J. Adams, et al., Experimental and theoretical challenges in the search for the quark gluon plasma: the STAR Collaboration's critical assessment of the evidence from RHIC collisions, Nucl. Phys. A 757 (2005) 102–183, http://dx.doi.org/10.1016/j.nuclphysa.2005.03.085, arXiv:nucl-ex/0501009.

[13] K. Aamodt, et al., Suppression of charged particle production at large transverse momentum in central Pb–Pb collisions at $\sqrt{s_{NN}} = 2.76$ TeV, Phys. Lett. B 696 (2011) 30–39, http://dx.doi.org/10.1016/j.physletb.2010.12.020, arXiv:1012.1004.

[14] S. Chatrchyan, et al., Study of high-pT charged particle suppression in PbPb compared to pp collisions at $\sqrt{s_{NN}} = 2.76$ TeV, Eur. Phys. J. C 72 (2012) 1945, http://dx.doi.org/10.1140/epjc/s10052-012-1945-x, arXiv:1202.2554.

[15] P. Abreu, et al., Identified charged particles in quark and gluon jets, Eur. Phys. J. C 17 (2000) 207–222, http://dx.doi.org/10.1007/s100520000449, arXiv:hep-ex/0106063.

[16] X.-N. Wang, Effect of jet quenching on high p_T hadron spectra in high-energy nuclear collisions, Phys. Rev. C 58 (1998) 2321, http://dx.doi.org/10.1103/PhysRevC.58.2321, arXiv:hep-ph/9804357.

[17] T. Renk, K.J. Eskola, Proton–antiproton suppression in 200A GeV Au–Au collisions, Phys. Rev. C 76 (2007) 027901, http://dx.doi.org/10.1103/PhysRevC.76.027901, arXiv:hep-ph/0702096.

[18] B. Abelev, et al., K^0_S and Λ production in Pb–Pb collisions at $\sqrt{s_{NN}} = 2.76$ TeV, Phys. Rev. Lett. 111 (2013) 222301, http://dx.doi.org/10.1103/PhysRevLett.111.222301, arXiv:1307.5530.

[19] S. Sapeta, U.A. Wiedemann, Jet hadrochemistry as a characteristics of jet quenching, Eur. Phys. J. C 55 (2008) 293–302, http://dx.doi.org/10.1140/epjc/s10052-008-0592-8, arXiv:0707.3494.

[20] P. Aurenche, B. Zakharov, Jet color chemistry and anomalous baryon production in AA-collisions, Eur. Phys. J. C 71 (2011) 1829, http://dx.doi.org/10.1140/epjc/s10052-011-1829-5, arXiv:1109.6819.

[21] R. Bellwied, C. Markert, In-medium hadronization in the deconfined matter at RHIC and LHC, Phys. Lett. B 691 (2010) 208–213, http://dx.doi.org/10.1016/j.physletb.2010.06.028, arXiv:1005.5416.

[22] B. Abelev, et al., Identified baryon and meson distributions at large transverse momenta from Au + Au collisions at $\sqrt{s_{NN}} = 200$, Phys. Rev. Lett. 97 (2006) 152301, http://dx.doi.org/10.1103/PhysRevLett.97.152301, arXiv:nucl-ex/0606003.

[23] G. Agakishiev, et al., Identified hadron compositions in p + p and Au + Au collisions at high transverse momenta at $\sqrt{s_{NN}} = 200$ GeV, Phys. Rev. Lett. 108 (2012) 072302, http://dx.doi.org/10.1103/PhysRevLett.108.072302, arXiv:1110.0579.

[24] A. Adare, et al., Spectra and ratios of identified particles in Au + Au and d + Au collisions at $\sqrt{s_{NN}} = 200$ GeV, Phys. Rev. C 88 (2013) 024906, http://dx.doi.org/10.1103/PhysRevC.88.024906, arXiv:1304.3410.

[25] K. Aamodt, et al., The ALICE experiment at the CERN LHC, J. Instrum. 3 (2008) S08002, http://dx.doi.org/10.1088/1748-0221/3/08/S08002.

[26] B. Abelev, et al., Centrality dependence of π, K, p production in Pb–Pb collisions at $\sqrt{s_{NN}} = 2.76$ TeV, Phys. Rev. C 88 (2013) 044910, http://dx.doi.org/10.1103/PhysRevC.88.044910, arXiv:1303.0737.

[27] K. Aamodt, et al., Production of pions, kaons and protons in pp collisions at $\sqrt{s} = 900$ GeV with ALICE at the LHC, Eur. Phys. J. C 71 (2011) 1655, http://dx.doi.org/10.1140/epjc/s10052-011-1655-9, arXiv:1101.4110.

[28] B. Abelev, et al., Measurement of inelastic, single- and double-diffraction cross sections in proton–proton collisions at the LHC with ALICE, Eur. Phys. J. C 73 (2013) 2456, http://dx.doi.org/10.1140/epjc/s10052-013-2456-0, arXiv:1208.4968.

[29] B. Abelev, et al., Centrality determination of Pb–Pb collisions at $\sqrt{s_{NN}} =$ 2.76 TeV with ALICE, Phys. Rev. C 88 (2013) 044909, http://dx.doi.org/10.1103/PhysRevC.88.044909, arXiv:1301.4361.

[30] E. Abbas, et al., Performance of the ALICE VZERO system, J. Instrum. 8 (2013) P10016, http://dx.doi.org/10.1088/1748-0221/8/10/P10016, arXiv:1306.3130.

[31] B. Abelev, et al., Centrality dependence of charged particle production at large transverse momentum in Pb–Pb collisions at $\sqrt{s_{\rm NN}} = 2.76$ TeV, Phys. Lett. B 720 (2013) 52–62, http://dx.doi.org/10.1016/j.physletb.2013.01.051, arXiv:1208.2711.

[32] ALICE Collaboration, ALICE Technical Design Report of the High Momentum Particle Identification Detector, CERN/LHCC 98-19, ALICE TDR 1.

[33] P. Martinengo, et al., The ALICE high momentum particle identification system: an overview after the first Large Hadron Collider run, Nucl. Instrum. Methods Phys. Res., Sect. A, Accel. Spectrom. Detect. Assoc. Equip. 639 (2011) 7–10, http://dx.doi.org/10.1016/j.nima.2010.10.038.

[34] D. Cozza, D. Di Bari, D. Elia, E. Nappi, A. Di Mauro, et al., Recognition of Cherenkov patterns in high multiplicity environments, Nucl. Instrum. Methods 482 (2002) 226–237, http://dx.doi.org/10.1016/S0168-9002(01)01625-4.

[35] B. Alessandro, et al., ALICE: physics performance report, vol. II, J. Phys. G 32 (2006) 1295–2040, http://dx.doi.org/10.1088/0954-3899/32/10/001.

[36] J. Alme, Y. Andres, H. Appelshauser, S. Bablok, N. Bialas, et al., The ALICE TPC, a large 3-dimensional tracking device with fast readout for ultra-high multiplicity events, Nucl. Instrum. Methods 622 (2010) 316–367, http://dx.doi.org/10.1016/j.nima.2010.04.042, arXiv:1001.1950.

[37] B.B. Abelev, et al., Energy dependence of the transverse momentum distributions of charged particles in pp collisions measured by ALICE, Eur. Phys. J. C 73 (2013) 2662, http://dx.doi.org/10.1140/epjc/s10052-013-2662-9, arXiv:1307.1093.

[38] P. Bozek, I. Wyskiel-Piekarska, Particle spectra in Pb–Pb collisions at $\sqrt{s_{NN}} = 2.76$ TeV, Phys. Rev. C 85 (2012) 064915, http://dx.doi.org/10.1103/PhysRevC.85.064915, arXiv:1203.6513.

[39] I. Karpenko, Y. Sinyukov, K. Werner, Uniform description of bulk observables in hydrokinetic model of A + A collisions at RHIC and LHC, Phys. Rev. C 87 (2013) 024914, http://dx.doi.org/10.1103/PhysRevC.87.024914, arXiv:1204.5351.

[40] K. Werner, I. Karpenko, M. Bleicher, T. Pierog, S. Porteboeuf-Houssais, Jets, bulk matter, and their interaction in heavy ion collisions at several tev, Phys. Rev. C 85 (2012) 064907, http://dx.doi.org/10.1103/PhysRevC.85.064907.

[41] K. Werner, Lambda-to-kaon ratio enhancement in heavy ion collisions at several TeV, Phys. Rev. Lett. 109 (2012) 102301, http://dx.doi.org/10.1103/PhysRevLett.109.102301.

[42] B.B. Abelev, et al., $K^*(892)^0$ and $\Phi(1020)$ production in Pb–Pb collisions at $\sqrt{s_{NN}} = 2.76$ TeV, arXiv:1404.0495.

[43] R. Sassot, P. Zurita, M. Stratmann, Inclusive hadron production in the CERN–LHC era, Phys. Rev. D 82 (2010) 074011, http://dx.doi.org/10.1103/PhysRevD.82.074011.

[44] D. d'Enterria, K.J. Eskola, I. Helenius, H. Paukkunen, Confronting current NLO parton fragmentation functions with inclusive charged-particle spectra at hadron colliders, arXiv:1311.1415.

ALICE Collaboration

B. Abelev [bt], J. Adam [ak], D. Adamová [cb], M.M. Aggarwal [cf], G. Aglieri Rinella [ah], M. Agnello [cm,dd], A. Agostinelli [z], N. Agrawal [ar], Z. Ahammed [dw], N. Ahmad [r], A. Ahmad Masoodi [r], I. Ahmed [o], S.U. Ahn [bm], S.A. Ahn [bm], I. Aimo [cm,dd], S. Aiola [eb], M. Ajaz [o], A. Akindinov [bc], D. Aleksandrov [cs], B. Alessandro [dd], D. Alexandre [cu], A. Alici [cx,l], A. Alkin [c], J. Alme [ai], T. Alt [am], V. Altini [ae], S. Altinpinar [q], I. Altsybeev [dv], C. Alves Garcia Prado [dl], C. Andrei [bw], A. Andronic [cp], V. Anguelov [cl], J. Anielski [ay], T. Antičić [cq], F. Antinori [da], P. Antonioli [cx], L. Aphecetche [df], H. Appelshäuser [aw], N. Arbor [bp], S. Arcelli [z], N. Armesto [p], R. Arnaldi [dd], T. Aronsson [eb], I.C. Arsene [u,cp], M. Arslandok [aw], A. Augustinus [ah], R. Averbeck [cp], T.C. Awes [cc], M.D. Azmi [r,ch], M. Bach [am], A. Badalà [cz], Y.W. Baek [an,bo], S. Bagnasco [dd], R. Bailhache [aw], V. Bairathi [cj], R. Bala [ci], A. Baldisseri [n], F. Baltasar Dos Santos Pedrosa [ah], J. Bán [bd], R.C. Baral [bf], R. Barbera [aa], F. Barile [ae], G.G. Barnaföldi [ea], L.S. Barnby [cu], V. Barret [bo], J. Bartke [di], M. Basile [z], N. Bastid [bo], S. Basu [dw], B. Bathen [ay], G. Batigne [df], B. Batyunya [bk], P.C. Batzing [u], C. Baumann [aw], I.G. Bearden [by], H. Beck [aw], C. Bedda [cm], N.K. Behera [ar], I. Belikov [az], F. Bellini [z], R. Bellwied [dn], E. Belmont-Moreno [bi], G. Bencedi [ea], S. Beole [y], I. Berceanu [bw], A. Bercuci [bw], Y. Berdnikov [cd,1], D. Berenyi [ea], M.E. Berger [ck], R.A. Bertens [bb], D. Berzano [y], L. Betev [ah], A. Bhasin [ci], A.K. Bhati [cf], B. Bhattacharjee [ao], J. Bhom [ds], L. Bianchi [y], N. Bianchi [bq], C. Bianchin [bb], J. Bielčík [ak], J. Bielčíková [cb], A. Bilandzic [by], S. Bjelogrlic [bb], F. Blanco [j], D. Blau [cs], C. Blume [aw], F. Bock [cl,bs], A. Bogdanov [bu], H. Bøggild [by], M. Bogolyubsky [de], F.V. Böhmer [ck], L. Boldizsár [ea], M. Bombara [al], J. Book [aw], H. Borel [n], A. Borissov [dz,co], J. Bornschein [am], F. Bossú [bj], M. Botje [bz], E. Botta [y], S. Böttger [av], P. Braun-Munzinger [cp], M. Bregant [dl], T. Breitner [av], T.A. Broker [aw], T.A. Browning [cn], M. Broz [aj,ak], E. Bruna [dd], G.E. Bruno [ae], D. Budnikov [cr], H. Buesching [aw], S. Bufalino [dd], P. Buncic [ah], O. Busch [cl], Z. Buthelezi [bj], D. Caffarri [ab], X. Cai [g], H. Caines [eb], A. Caliva [bb], E. Calvo Villar [cv], P. Camerini [x], V. Canoa Roman [ah], F. Carena [ah], W. Carena [ah], F. Carminati [ah], A. Casanova Díaz [bq], J. Castillo Castellanos [n], E.A.R. Casula [w], V. Catanescu [bw], C. Cavicchioli [ah], C. Ceballos Sanchez [i], J. Cepila [ak], P. Cerello [dd], B. Chang [do], S. Chapeland [ah], J.L. Charvet [n], S. Chattopadhyay [dw], S. Chattopadhyay [ct], M. Cherney [ce], C. Cheshkov [du], B. Cheynis [du], V. Chibante Barroso [ah], D.D. Chinellato [dn,dm], P. Chochula [ah], M. Chojnacki [by], S. Choudhury [dw], P. Christakoglou [bz], C.H. Christensen [by], P. Christiansen [af], T. Chujo [ds], S.U. Chung [co], C. Cicalo [cy], L. Cifarelli [l,z], F. Cindolo [cx], J. Cleymans [ch], F. Colamaria [ae], D. Colella [ae], A. Collu [w], M. Colocci [z], G. Conesa Balbastre [bp], Z. Conesa del Valle [au,ah], M.E. Connors [eb], G. Contin [x], J.G. Contreras [k], T.M. Cormier [cc,dz], Y. Corrales Morales [y], P. Cortese [ad], I. Cortés Maldonado [b], M.R. Cosentino [bs,dl], F. Costa [ah], P. Crochet [bo], R. Cruz Albino [k], E. Cuautle [bh], L. Cunqueiro [bq,ah], A. Dainese [da], R. Dang [g], A. Danu [bg], D. Das [ct], I. Das [au], K. Das [ct], S. Das [d], A. Dash [dm], S. Dash [ar], S. De [dw], H. Delagrange [df,2], A. Deloff [bv], E. Dénes [ea], G. D'Erasmo [ae], G.O.V. de Barros [dl], A. De Caro [l,ac], G. de Cataldo [cw], J. de Cuveland [am], A. De Falco [w], D. De Gruttola [ac,l], N. De Marco [dd], S. De Pasquale [ac], R. de Rooij [bb], M.A. Diaz Corchero [j], T. Dietel [ay,ch], R. Divià [ah], D. Di Bari [ae], S. Di Liberto [db], A. Di Mauro [ah], P. Di Nezza [bq], Ø. Djuvsland [q], A. Dobrin [bb], T. Dobrowolski [bv], D. Domenicis Gimenez [dl], B. Dönigus [aw], O. Dordic [u], S. Dørheim [ck], A.K. Dubey [dw], A. Dubla [bb], L. Ducroux [du], P. Dupieux [bo], A.K. Dutta Majumdar [ct], R.J. Ehlers [eb], D. Elia [cw], H. Engel [av], B. Erazmus [ah,df], H.A. Erdal [ai], D. Eschweiler [am], B. Espagnon [au], M. Estienne [df], S. Esumi [ds], D. Evans [cu], S. Evdokimov [de], G. Eyyubova [u], D. Fabris [da], J. Faivre [bp], D. Falchieri [z], A. Fantoni [bq], M. Fasel [cl], D. Fehlker [q], L. Feldkamp [ay], D. Felea [bg], A. Feliciello [dd], G. Feofilov [dv], J. Ferencei [cb], A. Fernández Téllez [b], E.G. Ferreiro [p], A. Ferretti [y], A. Festanti [ab], J. Figiel [di], M.A.S. Figueredo [dl,dp], S. Filchagin [cr], D. Finogeev [ba], F.M. Fionda [ae], E.M. Fiore [ae], E. Floratos [cg], M. Floris [ah], S. Foertsch [bj], P. Foka [cp], S. Fokin [cs], E. Fragiacomo [dc], A. Francescon [ab,ah], U. Frankenfeld [cp], U. Fuchs [ah], C. Furget [bp], M. Fusco Girard [ac], J.J. Gaardhøje [by], M. Gagliardi [y], A.M. Gago [cv], M. Gallio [y], D.R. Gangadharan [s,bs], P. Ganoti [cg,cc], C. Garabatos [cp], E. Garcia-Solis [m], C. Gargiulo [ah], I. Garishvili [bt], J. Gerhard [am], M. Germain [df], A. Gheata [ah], M. Gheata [bg,ah], B. Ghidini [ae], P. Ghosh [dw], S.K. Ghosh [d], P. Gianotti [bq], P. Giubellino [ah], E. Gladysz-Dziadus [di], P. Glässel [cl], R. Gomez [k], P. González-Zamora [j], S. Gorbunov [am], L. Görlich [di], S. Gotovac [dh], L.K. Graczykowski [dy], R. Grajcarek [cl], A. Grelli [bb], A. Grigoras [ah], C. Grigoras [ah], V. Grigoriev [bu], A. Grigoryan [a], S. Grigoryan [bk], B. Grinyov [c], N. Grion [dc], J.F. Grosse-Oetringhaus [ah], J.-Y. Grossiord [du], R. Grosso [ah], F. Guber [ba], R. Guernane [bp], B. Guerzoni [z], M. Guilbaud [du], K. Gulbrandsen [by], H. Gulkanyan [a], T. Gunji [dr], A. Gupta [ci], R. Gupta [ci], K.H. Khan [o], R. Haake [ay], Ø. Haaland [q], C. Hadjidakis [au], M. Haiduc [bg], H. Hamagaki [dr], G. Hamar [ea], L.D. Hanratty [cu], A. Hansen [by], J.W. Harris [eb], H. Hartmann [am], A. Harton [m], D. Hatzifotiadou [cx], S. Hayashi [dr], S.T. Heckel [aw],

M. Heide [ay], H. Helstrup [ai], A. Herghelegiu [bw], G. Herrera Corral [k], B.A. Hess [ag], K.F. Hetland [ai], B. Hicks [eb], B. Hippolyte [az], J. Hladky [be], P. Hristov [ah], M. Huang [q], T.J. Humanic [s], D. Hutter [am], D.S. Hwang [t], R. Ilkaev [cr], I. Ilkiv [bv], M. Inaba [ds], E. Incani [w], G.M. Innocenti [y], C. Ionita [ah], M. Ippolitov [cs], M. Irfan [r], M. Ivanov [cp], V. Ivanov [cd], O. Ivanytskyi [c], A. Jachołkowski [aa], P.M. Jacobs [bs], C. Jahnke [dl], H.J. Jang [bm], M.A. Janik [dy], P.H.S.Y. Jayarathna [dn], S. Jena [ar,dn], R.T. Jimenez Bustamante [bh], P.G. Jones [cu], H. Jung [an], A. Jusko [cu], S. Kalcher [am], P. Kalinak [bd], A. Kalweit [ah], J. Kamin [aw], J.H. Kang [ec], V. Kaplin [bu], S. Kar [dw], A. Karasu Uysal [bn], O. Karavichev [ba], T. Karavicheva [ba], E. Karpechev [ba], U. Kebschull [av], R. Keidel [ed], B. Ketzer [ck], M.M. Khan [r,3], P. Khan [ct], S.A. Khan [dw], A. Khanzadeev [cd], Y. Kharlov [de], B. Kileng [ai], B. Kim [ec], D.W. Kim [bm,an], D.J. Kim [do], J.S. Kim [an], M. Kim [an], M. Kim [ec], S. Kim [t], T. Kim [ec], S. Kirsch [am], I. Kisel [am], S. Kiselev [bc], A. Kisiel [dy], G. Kiss [ea], J.L. Klay [f], J. Klein [cl], C. Klein-Bösing [ay], A. Kluge [ah], M.L. Knichel [cp], A.G. Knospe [dj], C. Kobdaj [ah,dg], M. Kofarago [ah], M.K. Köhler [cp], T. Kollegger [am], A. Kolojvari [dv], V. Kondratiev [dv], N. Kondratyeva [bu], A. Konevskikh [ba], V. Kovalenko [dv], M. Kowalski [ah,di], S. Kox [bp], G. Koyithatta Meethaleveedu [ar], J. Kral [do], I. Králik [bd], F. Kramer [aw], A. Kravčáková [al], M. Krelina [ak], M. Kretz [am], M. Krivda [cu,bd], F. Krizek [cb,ap], M. Krus [ak], E. Kryshen [cd,ah], M. Krzewicki [cp], V. Kučera [cb], Y. Kucheriaev [cs,2], T. Kugathasan [ah], C. Kuhn [az], P.G. Kuijer [bz], I. Kulakov [aw], J. Kumar [ar], P. Kurashvili [bv], A. Kurepin [ba], A.B. Kurepin [ba], A. Kuryakin [cr], S. Kushpil [cb], V. Kushpil [cb], M.J. Kweon [cl,at], Y. Kwon [ec], P. Ladron de Guevara [bh], C. Lagana Fernandes [dl], I. Lakomov [au], R. Langoy [dx], C. Lara [av], A. Lardeux [df], A. Lattuca [y], S.L. La Pointe [dd,bb], P. La Rocca [aa], R. Lea [x], L. Leardini [cl], G.R. Lee [cu], I. Legrand [ah], J. Lehnert [aw], R.C. Lemmon [ca], M. Lenhardt [cp], V. Lenti [cw], E. Leogrande [bb], M. Leoncino [y], I. León Monzón [dk], P. Lévai [ea], S. Li [g,bo], J. Lien [dx], R. Lietava [cu], S. Lindal [u], V. Lindenstruth [am], C. Lippmann [cp], M.A. Lisa [s], H.M. Ljunggren [af], D.F. Lodato [bb], P.I. Loenne [q], V.R. Loggins [dz], V. Loginov [bu], D. Lohner [cl], C. Loizides [bs], X. Lopez [bo], E. López Torres [i], X.-G. Lu [cl], P. Luettig [aw], M. Lunardon [ab], J. Luo [g], G. Luparello [bb], C. Luzzi [ah], R. Ma [eb], A. Maevskaya [ba], M. Mager [ah], D.P. Mahapatra [bf], A. Maire [cl,az], M. Malaev [cd], I. Maldonado Cervantes [bh], L. Malinina [bk,4], D. Mal'Kevich [bc], P. Malzacher [cp], A. Mamonov [cr], L. Manceau [dd], V. Manko [cs], F. Manso [bo], V. Manzari [ah,cw], M. Marchisone [y,bo], J. Mareš [be], G.V. Margagliotti [x], A. Margotti [cx], A. Marín [cp], C. Markert [ah,dj], M. Marquard [aw], I. Martashvili [dq], N.A. Martin [cp], P. Martinengo [ah], M.I. Martínez [b], G. Martínez García [df], J. Martin Blanco [df], Y. Martynov [c], A. Mas [df], S. Masciocchi [cp], M. Masera [y], A. Masoni [cy], L. Massacrier [df], A. Mastroserio [ae], A. Matyja [di], C. Mayer [di], J. Mazer [dq], R. Mazumder [as], M.A. Mazzoni [db], F. Meddi [v], A. Menchaca-Rocha [bi], E. Meninno [ac], J. Mercado Pérez [cl], M. Meres [aj], Y. Miake [ds], K. Mikhaylov [bc,bk], L. Milano [ah], J. Milosevic [u,5], A. Mischke [bb], A.N. Mishra [as], D. Miśkowiec [cp], C.M. Mitu [bg], J. Mlynarz [dz], B. Mohanty [dw,bx], L. Molnar [az], L. Montaño Zetina [k], E. Montes [j], M. Morando [ab], D.A. Moreira De Godoy [dl], S. Moretto [ab], A. Morreale [do,df], A. Morsch [ah], V. Muccifora [bq], E. Mudnic [dh], S. Muhuri [dw], M. Mukherjee [dw], H. Müller [ah], M.G. Munhoz [dl], S. Murray [ch], L. Musa [ah], J. Musinsky [bd], B.K. Nandi [ar], R. Nania [cx], E. Nappi [cw], C. Nattrass [dq], T.K. Nayak [dw], S. Nazarenko [cr], A. Nedosekin [bc], M. Nicassio [cp], M. Niculescu [bg,ah], B.S. Nielsen [by], S. Nikolaev [cs], S. Nikulin [cs], V. Nikulin [cd], B.S. Nilsen [ce], F. Noferini [l,cx], P. Nomokonov [bk], G. Nooren [bb], A. Nyanin [cs], J. Nystrand [q], H. Oeschler [cl,ax], S. Oh [eb], S.K. Oh [bl,an,6], A. Okatan [bn], L. Olah [ea], J. Oleniacz [dy], A.C. Oliveira Da Silva [dl], J. Onderwaater [cp], C. Oppedisano [dd], A. Ortiz Velasquez [af], A. Oskarsson [af], J. Otwinowski [cp], K. Oyama [cl], Y. Pachmayer [cl], M. Pachr [ak], P. Pagano [ac], G. Paić [bh], F. Painke [am], C. Pajares [p], S.K. Pal [dw], A. Palmeri [cz], D. Pant [ar], V. Papikyan [a], G.S. Pappalardo [cz], W.J. Park [cp], A. Passfeld [ay], D.I. Patalakha [de], V. Paticchio [cw], B. Paul [ct], T. Pawlak [dy], T. Peitzmann [bb], H. Pereira Da Costa [n], E. Pereira De Oliveira Filho [dl], D. Peresunko [cs], C.E. Pérez Lara [bz], W. Peryt [dy,2], A. Pesci [cx], Y. Pestov [e], V. Petráček [ak], M. Petran [ak], M. Petris [bw], M. Petrovici [bw], C. Petta [aa], S. Piano [dc], M. Pikna [aj], P. Pillot [df], O. Pinazza [ah,cx], L. Pinsky [dn], D.B. Piyarathna [dn], M. Płoskoń [bs], M. Planinic [cq,dt], J. Pluta [dy], S. Pochybova [ea], P.L.M. Podesta-Lerma [dk], M.G. Poghosyan [ah,ce], E.H.O. Pohjoisaho [ap], B. Polichtchouk [de], N. Poljak [cq,dt], A. Pop [bw], S. Porteboeuf-Houssais [bo], J. Porter [bs], V. Pospisil [ak], B. Potukuchi [ci], S.K. Prasad [d,dz], R. Preghenella [cx,l], F. Prino [dd], C.A. Pruneau [dz], I. Pshenichnov [ba], G. Puddu [w], V. Punin [cr], J. Putschke [dz], H. Qvigstad [u], A. Rachevski [dc], S. Raha [d], J. Rak [do], A. Rakotozafindrabe [n], L. Ramello [ad], R. Raniwala [cj], S. Raniwala [cj], S.S. Räsänen [ap], B.T. Rascanu [aw], D. Rathee [cf], A.W. Rauf [o], V. Razazi [w], K.F. Read [dq], J.S. Real [bp], K. Redlich [bv,7], R.J. Reed [eb], A. Rehman [q], P. Reichelt [aw], M. Reicher [bb], F. Reidt [cl,ah], R. Renfordt [aw], A.R. Reolon [bq], A. Reshetin [ba], F. Rettig [am], J.-P. Revol [ah], K. Reygers [cl], V. Riabov [cd], R.A. Ricci [br], T. Richert [af], M. Richter [u], P. Riedler [ah], W. Riegler [ah], F. Riggi [aa], A. Rivetti [dd], E. Rocco [bb],

M. Rodríguez Cahuantzi [b], A. Rodriguez Manso [bz], K. Røed [u], E. Rogochaya [bk], S. Rohni [ci], D. Rohr [am], D. Röhrich [q], R. Romita [dp,ca], F. Ronchetti [bq], L. Ronflette [df], P. Rosnet [bo], S. Rossegger [ah], A. Rossi [ah], F. Roukoutakis [cg,ah], A. Roy [as], C. Roy [az], P. Roy [ct], A.J. Rubio Montero [j], R. Rui [x], R. Russo [y], E. Ryabinkin [cs], Y. Ryabov [cd], A. Rybicki [di], S. Sadovsky [de], K. Šafařík [ah], B. Sahlmuller [aw], R. Sahoo [as], P.K. Sahu [bf], J. Saini [dw], C.A. Salgado [p], J. Salzwedel [s], S. Sambyal [ci], V. Samsonov [cd], X. Sanchez Castro [az,bh], F.J. Sánchez Rodríguez [dk], L. Šándor [bd], A. Sandoval [bi], M. Sano [ds], G. Santagati [aa], D. Sarkar [dw], E. Scapparone [cx], F. Scarlassara [ab], R.P. Scharenberg [cn], C. Schiaua [bw], R. Schicker [cl], C. Schmidt [cp], H.R. Schmidt [ag], S. Schuchmann [aw], J. Schukraft [ah], M. Schulc [ak], T. Schuster [eb], Y. Schutz [ah,df], K. Schwarz [cp], K. Schweda [cp], G. Scioli [z], E. Scomparin [dd], P.A. Scott [cu], R. Scott [dq], G. Segato [ab], J.E. Seger [ce], I. Selyuzhenkov [cp], J. Seo [co], E. Serradilla [j,bi], A. Sevcenco [bg], A. Shabetai [df], G. Shabratova [bk], R. Shahoyan [ah], A. Shangaraev [de], N. Sharma [dq,bf], S. Sharma [ci], K. Shigaki [aq], K. Shtejer [y], Y. Sibiriak [cs], S. Siddhanta [cy], T. Siemiarczuk [bv], D. Silvermyr [cc], C. Silvestre [bp], G. Simatovic [dt], R. Singaraju [dw], R. Singh [ci], S. Singha [bx,dw], V. Singhal [dw], B.C. Sinha [dw], T. Sinha [ct], B. Sitar [aj], M. Sitta [ad], T.B. Skaali [u], K. Skjerdal [q], R. Smakal [ak], N. Smirnov [eb], R.J.M. Snellings [bb], C. Søgaard [af], R. Soltz [bt], J. Song [co], M. Song [ec], F. Soramel [ab], S. Sorensen [dq], M. Spacek [ak], I. Sputowska [di], M. Spyropoulou-Stassinaki [cg], B.K. Srivastava [cn], J. Stachel [cl], I. Stan [bg], G. Stefanek [bv], M. Steinpreis [s], E. Stenlund [af], G. Steyn [bj], J.H. Stiller [cl], D. Stocco [df], M. Stolpovskiy [de], P. Strmen [aj], A.A.P. Suaide [dl], M.A. Subieta Vasquez [y], T. Sugitate [aq], C. Suire [au], M. Suleymanov [o], R. Sultanov [bc], M. Šumbera [cb], T. Susa [cq], T.J.M. Symons [bs], A. Szanto de Toledo [dl], I. Szarka [aj], A. Szczepankiewicz [ah], M. Szymanski [dy], J. Takahashi [dm], M.A. Tangaro [ae], J.D. Tapia Takaki [au,8], A. Tarantola Peloni [aw], A. Tarazona Martinez [ah], M.G. Tarzila [bw], A. Tauro [ah], G. Tejeda Muñoz [b], A. Telesca [ah], C. Terrevoli [w], A. Ter Minasyan [bu], J. Thäder [cp], D. Thomas [bb], R. Tieulent [du], A.R. Timmins [dn], A. Toia [da,aw], H. Torii [dr], V. Trubnikov [c], W.H. Trzaska [do], T. Tsuji [dr], A. Tumkin [cr], R. Turrisi [da], T.S. Tveter [u], J. Ulery [aw], K. Ullaland [q], A. Uras [du], G.L. Usai [w], M. Vajzer [cb], M. Vala [bk,bd], L. Valencia Palomo [au,bo], S. Vallero [y,cl], P. Vande Vyvre [ah], L. Vannucci [br], J. Van Der Maarel [bb], J.W. Van Hoorne [ah], M. van Leeuwen [bb], A. Vargas [b], R. Varma [ar], M. Vasileiou [cg], A. Vasiliev [cs], V. Vechernin [dv], M. Veldhoen [bb], A. Velure [q], M. Venaruzzo [x], E. Vercellin [y], S. Vergara Limón [b], R. Vernet [h], M. Verweij [dz], L. Vickovic [dh], G. Viesti [ab], J. Viinikainen [do], Z. Vilakazi [bj], O. Villalobos Baillie [cu], A. Vinogradov [cs], L. Vinogradov [dv], Y. Vinogradov [cr], T. Virgili [ac], Y.P. Viyogi [dw], A. Vodopyanov [bk], M.A. Völkl [cl], K. Voloshin [bc], S.A. Voloshin [dz], G. Volpe [ah], B. von Haller [ah], I. Vorobyev [dv], D. Vranic [cp,ah], J. Vrláková [al], B. Vulpescu [bo], A. Vyushin [cr], B. Wagner [q], J. Wagner [cp], V. Wagner [ak], M. Wang [g,df], Y. Wang [cl], D. Watanabe [ds], M. Weber [dn], J.P. Wessels [ay], U. Westerhoff [ay], J. Wiechula [ag], J. Wikne [u], M. Wilde [ay], G. Wilk [bv], J. Wilkinson [cl], M.C.S. Williams [cx], B. Windelband [cl], M. Winn [cl], C. Xiang [g], C.G. Yaldo [dz], Y. Yamaguchi [dr], H. Yang [bb], P. Yang [g], S. Yang [q], S. Yano [aq], S. Yasnopolskiy [cs], J. Yi [co], Z. Yin [g], I.-K. Yoo [co], I. Yushmanov [cs], V. Zaccolo [by], C. Zach [ak], A. Zaman [o], C. Zampolli [cx], S. Zaporozhets [bk], A. Zarochentsev [dv], P. Závada [be], N. Zaviyalov [cr], H. Zbroszczyk [dy], I.S. Zgura [bg], M. Zhalov [cd], F. Zhang [g], H. Zhang [g], X. Zhang [bo,g,bs], Y. Zhang [g], C. Zhao [u], D. Zhou [g], F. Zhou [g], Y. Zhou [bb], H. Zhu [g], J. Zhu [df,g], J. Zhu [g], X. Zhu [g], A. Zichichi [l,z], A. Zimmermann [cl], M.B. Zimmermann [ay,ah], G. Zinovjev [c], Y. Zoccarato [du], M. Zynovyev [c], M. Zyzak [aw]

[a] *A.I. Alikhanyan National Science Laboratory (Yerevan Physics Institute) Foundation, Yerevan, Armenia*
[b] *Benemérita Universidad Autónoma de Puebla, Puebla, Mexico*
[c] *Bogolyubov Institute for Theoretical Physics, Kiev, Ukraine*
[d] *Bose Institute, Department of Physics and Centre for Astroparticle Physics and Space Science (CAPSS), Kolkata, India*
[e] *Budker Institute for Nuclear Physics, Novosibirsk, Russia*
[f] *California Polytechnic State University, San Luis Obispo, CA, United States*
[g] *Central China Normal University, Wuhan, China*
[h] *Centre de Calcul de l'IN2P3, Villeurbanne, France*
[i] *Centro de Aplicaciones Tecnológicas y Desarrollo Nuclear (CEADEN), Havana, Cuba*
[j] *Centro de Investigaciones Energéticas Medioambientales y Tecnológicas (CIEMAT), Madrid, Spain*
[k] *Centro de Investigación y de Estudios Avanzados (CINVESTAV), Mexico City and Mérida, Mexico*
[l] *Centro Fermi – Museo Storico della Fisica e Centro Studi e Ricerche "Enrico Fermi", Rome, Italy*
[m] *Chicago State University, Chicago, USA*
[n] *Commissariat à l'Energie Atomique, IRFU, Saclay, France*
[o] *COMSATS Institute of Information Technology (CIIT), Islamabad, Pakistan*
[p] *Departamento de Física de Partículas and IGFAE, Universidad de Santiago de Compostela, Santiago de Compostela, Spain*
[q] *Department of Physics and Technology, University of Bergen, Bergen, Norway*
[r] *Department of Physics, Aligarh Muslim University, Aligarh, India*
[s] *Department of Physics, Ohio State University, Columbus, OH, United States*
[t] *Department of Physics, Sejong University, Seoul, South Korea*
[u] *Department of Physics, University of Oslo, Oslo, Norway*
[v] *Dipartimento di Fisica dell'Università 'La Sapienza' and Sezione INFN Rome, Italy*

[w] Dipartimento di Fisica dell'Università and Sezione INFN, Cagliari, Italy
[x] Dipartimento di Fisica dell'Università and Sezione INFN, Trieste, Italy
[y] Dipartimento di Fisica dell'Università and Sezione INFN, Turin, Italy
[z] Dipartimento di Fisica e Astronomia dell'Università and Sezione INFN, Bologna, Italy
[aa] Dipartimento di Fisica e Astronomia dell'Università and Sezione INFN, Catania, Italy
[ab] Dipartimento di Fisica e Astronomia dell'Università and Sezione INFN, Padova, Italy
[ac] Dipartimento di Fisica 'E.R. Caianiello' dell'Università and Gruppo Collegato INFN, Salerno, Italy
[ad] Dipartimento di Scienze e Innovazione Tecnologica dell'Università del Piemonte Orientale and Gruppo Collegato INFN, Alessandria, Italy
[ae] Dipartimento Interateneo di Fisica 'M. Merlin' and Sezione INFN, Bari, Italy
[af] Division of Experimental High Energy Physics, University of Lund, Lund, Sweden
[ag] Eberhard Karls Universität Tübingen, Tübingen, Germany
[ah] European Organization for Nuclear Research (CERN), Geneva, Switzerland
[ai] Faculty of Engineering, Bergen University College, Bergen, Norway
[aj] Faculty of Mathematics, Physics and Informatics, Comenius University, Bratislava, Slovakia
[ak] Faculty of Nuclear Sciences and Physical Engineering, Czech Technical University in Prague, Prague, Czech Republic
[al] Faculty of Science, P.J. Šafárik University, Košice, Slovakia
[am] Frankfurt Institute for Advanced Studies, Johann Wolfgang Goethe-Universität Frankfurt, Frankfurt, Germany
[an] Gangneung-Wonju National University, Gangneung, South Korea
[ao] Gauhati University, Department of Physics, Guwahati, India
[ap] Helsinki Institute of Physics (HIP), Helsinki, Finland
[aq] Hiroshima University, Hiroshima, Japan
[ar] Indian Institute of Technology Bombay (IIT), Mumbai, India
[as] Indian Institute of Technology Indore (IITI), Indore, India
[at] Inha University, Incheon, South Korea
[au] Institut de Physique Nucléaire d'Orsay (IPNO), Université Paris-Sud, CNRS-IN2P3, Orsay, France
[av] Institut für Informatik, Johann Wolfgang Goethe-Universität Frankfurt, Frankfurt, Germany
[aw] Institut für Kernphysik, Johann Wolfgang Goethe-Universität Frankfurt, Frankfurt, Germany
[ax] Institut für Kernphysik, Technische Universität Darmstadt, Darmstadt, Germany
[ay] Institut für Kernphysik, Westfälische Wilhelms-Universität Münster, Münster, Germany
[az] Institut Pluridisciplinaire Hubert Curien (IPHC), Université de Strasbourg, CNRS-IN2P3, Strasbourg, France
[ba] Institute for Nuclear Research, Academy of Sciences, Moscow, Russia
[bb] Institute for Subatomic Physics of Utrecht University, Utrecht, Netherlands
[bc] Institute for Theoretical and Experimental Physics, Moscow, Russia
[bd] Institute of Experimental Physics, Slovak Academy of Sciences, Košice, Slovakia
[be] Institute of Physics, Academy of Sciences of the Czech Republic, Prague, Czech Republic
[bf] Institute of Physics, Bhubaneswar, India
[bg] Institute of Space Science (ISS), Bucharest, Romania
[bh] Instituto de Ciencias Nucleares, Universidad Nacional Autónoma de México, Mexico City, Mexico
[bi] Instituto de Física, Universidad Nacional Autónoma de México, Mexico City, Mexico
[bj] iThemba LABS, National Research Foundation, Somerset West, South Africa
[bk] Joint Institute for Nuclear Research (JINR), Dubna, Russia
[bl] Konkuk University, Seoul, South Korea
[bm] Korea Institute of Science and Technology Information, Daejeon, South Korea
[bn] KTO Karatay University, Konya, Turkey
[bo] Laboratoire de Physique Corpusculaire (LPC), Clermont Université, Université Blaise Pascal, CNRS-IN2P3, Clermont-Ferrand, France
[bp] Laboratoire de Physique Subatomique et de Cosmologie (LPSC), Université Joseph Fourier, CNRS-IN2P3, Institut Polytechnique de Grenoble, Grenoble, France
[bq] Laboratori Nazionali di Frascati, INFN, Frascati, Italy
[br] Laboratori Nazionali di Legnaro, INFN, Legnaro, Italy
[bs] Lawrence Berkeley National Laboratory, Berkeley, CA, United States
[bt] Lawrence Livermore National Laboratory, Livermore, CA, United States
[bu] Moscow Engineering Physics Institute, Moscow, Russia
[bv] National Centre for Nuclear Studies, Warsaw, Poland
[bw] National Institute for Physics and Nuclear Engineering, Bucharest, Romania
[bx] National Institute of Science Education and Research, Bhubaneswar, India
[by] Niels Bohr Institute, University of Copenhagen, Copenhagen, Denmark
[bz] Nikhef, National Institute for Subatomic Physics, Amsterdam, Netherlands
[ca] Nuclear Physics Group, STFC Daresbury Laboratory, Daresbury, United Kingdom
[cb] Nuclear Physics Institute, Academy of Sciences of the Czech Republic, Řež u Prahy, Czech Republic
[cc] Oak Ridge National Laboratory, Oak Ridge, TN, United States
[cd] Petersburg Nuclear Physics Institute, Gatchina, Russia
[ce] Physics Department, Creighton University, Omaha, NE, United States
[cf] Physics Department, Panjab University, Chandigarh, India
[cg] Physics Department, University of Athens, Athens, Greece
[ch] Physics Department, University of Cape Town, Cape Town, South Africa
[ci] Physics Department, University of Jammu, Jammu, India
[cj] Physics Department, University of Rajasthan, Jaipur, India
[ck] Physik Department, Technische Universität München, Munich, Germany
[cl] Physikalisches Institut, Ruprecht-Karls-Universität Heidelberg, Heidelberg, Germany
[cm] Politecnico di Torino, Turin, Italy
[cn] Purdue University, West Lafayette, IN, United States
[co] Pusan National University, Pusan, South Korea
[cp] Research Division and ExtreMe Matter Institute EMMI, GSI Helmholtzzentrum für Schwerionenforschung, Darmstadt, Germany
[cq] Rudjer Bošković Institute, Zagreb, Croatia
[cr] Russian Federal Nuclear Center (VNIIEF), Sarov, Russia
[cs] Russian Research Centre Kurchatov Institute, Moscow, Russia
[ct] Saha Institute of Nuclear Physics, Kolkata, India
[cu] School of Physics and Astronomy, University of Birmingham, Birmingham, United Kingdom
[cv] Sección Física, Departamento de Ciencias, Pontificia Universidad Católica del Perú, Lima, Peru
[cw] Sezione INFN, Bari, Italy

[cx] *Sezione INFN, Bologna, Italy*
[cy] *Sezione INFN, Cagliari, Italy*
[cz] *Sezione INFN, Catania, Italy*
[da] *Sezione INFN, Padova, Italy*
[db] *Sezione INFN, Rome, Italy*
[dc] *Sezione INFN, Trieste, Italy*
[dd] *Sezione INFN, Turin, Italy*
[de] *SSC IHEP of NRC "Kurchatov Institute", Protvino, Russia*
[df] *SUBATECH, Ecole des Mines de Nantes, Université de Nantes, CNRS-IN2P3, Nantes, France*
[dg] *Suranaree University of Technology, Nakhon Ratchasima, Thailand*
[dh] *Technical University of Split FESB, Split, Croatia*
[di] *The Henryk Niewodniczanski Institute of Nuclear Physics, Polish Academy of Sciences, Cracow, Poland*
[dj] *The University of Texas at Austin, Physics Department, Austin, TX, USA*
[dk] *Universidad Autónoma de Sinaloa, Culiacán, Mexico*
[dl] *Universidade de São Paulo (USP), São Paulo, Brazil*
[dm] *Universidade Estadual de Campinas (UNICAMP), Campinas, Brazil*
[dn] *University of Houston, Houston, TX, United States*
[do] *University of Jyväskylä, Jyväskylä, Finland*
[dp] *University of Liverpool, Liverpool, United Kingdom*
[dq] *University of Tennessee, Knoxville, TN, United States*
[dr] *University of Tokyo, Tokyo, Japan*
[ds] *University of Tsukuba, Tsukuba, Japan*
[dt] *University of Zagreb, Zagreb, Croatia*
[du] *Université de Lyon, Université Lyon 1, CNRS/IN2P3, IPN-Lyon, Villeurbanne, France*
[dv] *V. Fock Institute for Physics, St. Petersburg State University, St. Petersburg, Russia*
[dw] *Variable Energy Cyclotron Centre, Kolkata, India*
[dx] *Vestfold University College, Tonsberg, Norway*
[dy] *Warsaw University of Technology, Warsaw, Poland*
[dz] *Wayne State University, Detroit, MI, United States*
[ea] *Wigner Research Centre for Physics, Hungarian Academy of Sciences, Budapest, Hungary*
[eb] *Yale University, New Haven, CT, United States*
[ec] *Yonsei University, Seoul, South Korea*
[ed] *Zentrum für Technologietransfer und Telekommunikation (ZTT), Fachhochschule Worms, Worms, Germany*

[1] St. Petersburg State Polytechnical University.
[2] Deceased.
[3] Department of Applied Physics, Aligarh Muslim University, Aligarh, India.
[4] M.V. Lomonosov Moscow State University, D.V. Skobeltsyn Institute of Nuclear Physics, Moscow, Russia.
[5] University of Belgrade, Faculty of Physics and "Vinča" Institute of Nuclear Sciences, Belgrade, Serbia.
[6] Permanent Address: Konkuk University, Seoul, South Korea.
[7] Institute of Theoretical Physics, University of Wroclaw, Wroclaw, Poland.
[8] University of Kansas, Lawrence, KS, United States.